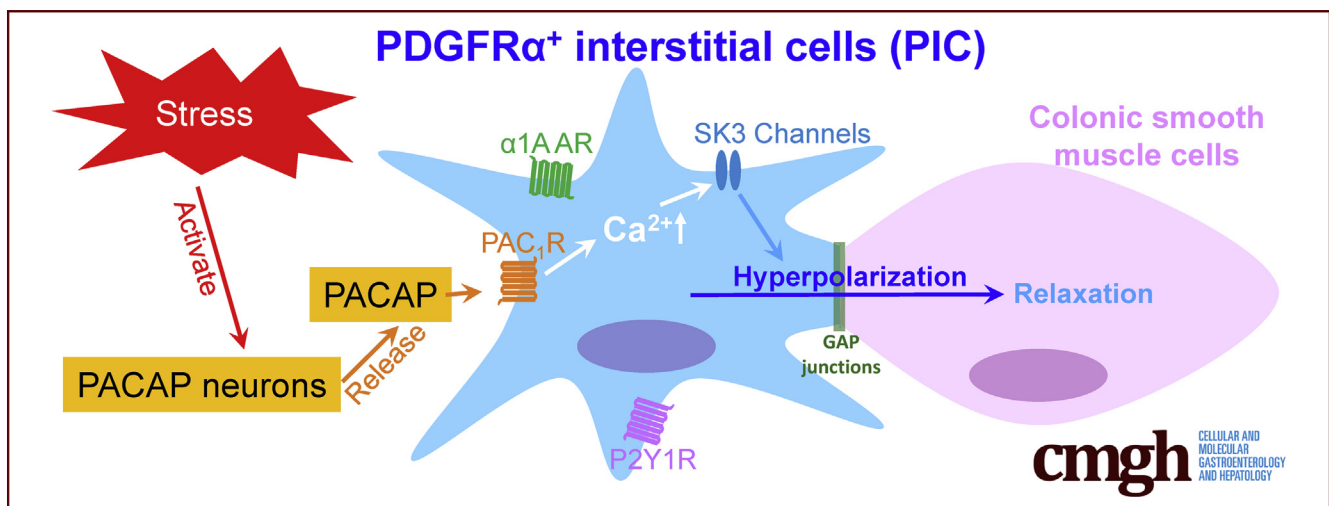


ORIGINAL RESEARCH

PDGFR α ⁺ Interstitial Cells are Effector Cells of PACAP Signaling in Mouse and Human ColonMasaaki Kurahashi,¹ Salah A. Baker,² Yoshihiko Kito,³ Allison Bartlett,² Masayasu Hara,⁴ Hiromitsu Takeyama,⁴ Hikaru Hashitani,⁵ and Kenton M. Sanders²

¹Department of Internal Medicine, Division of Gastroenterology and Hepatology, University of Iowa, Iowa City, Iowa, USA; ²Department of Physiology and Cell Biology, University of Nevada School of Medicine, Reno, Nevada, USA; ³Department of Pharmacology, Faculty of Medicine, Saga University, Saga, Japan; ⁴Department of Gastroenterological Surgery, Nagoya City University Graduate School of Medical Sciences, Nagoya, Japan; and ⁵Department of Cell Physiology, Nagoya City University Graduate School of Medical Sciences, Nagoya, Japan



SUMMARY

Platelet-derived growth factor receptor α -positive interstitial cells (PIC) inhibit colonic contractions through PAC₁R-SK channel signal pathway activated by pituitary adenylate cyclase-activating polypeptide in mouse and human colon. PIC integrate inhibitory inputs from several neurotransmitters to regulate colonic contractions. Further investigation of the functional roles of PIC in physiology and pathophysiology of colonic motility might lead to development of new treatments for functional bowel disorders.

BACKGROUND & AIMS: Platelet-derived growth factor receptor α (PDGFR α)-positive interstitial cells (PIC) are interposed between enteric nerve fibers and smooth muscle cells (SMCs) in the tunica muscularis of the gastrointestinal tract. PIC have robust expression of small conductance Ca²⁺ activated K⁺ channels 3 (SK3 channels) and transduce inhibitory inputs from purinergic and sympathetic nerves in mouse and human colon. We investigated whether PIC also express pituitary adenylate cyclase-activating polypeptide (PACAP) receptors, PAC1 (PAC₁R), and are involved in mediating inhibitory regulation of colonic contractions by PACAP in mouse and human colons.

METHODS: Gene expression analysis, Ca²⁺ imaging, and contractile experiments were performed on mouse colonic muscles. Ca²⁺ imaging, intracellular electrical recordings, and contractile experiments were performed on human colonic muscles.

RESULTS: *Adcyap1r1* (encoding PAC₁R) is highly expressed in mouse PIC. Interstitial cells of Cajal (ICC) and SMCs expressed far lower levels of *Adcyap1r1*. *Vipr1* and *Vipr2* were expressed at low levels in PIC, ICC, and SMCs. PACAP elicited Ca²⁺ transients in mouse PIC and inhibited spontaneous phasic contractions via SK channels. In human colonic muscles, PAC₁R agonists elicited Ca²⁺ transients in PIC, hyperpolarized SMCs through SK channels and inhibited spontaneous phasic contractions.

CONCLUSIONS: PIC of mouse and human colon utilize PAC₁R-SK channel signal pathway to inhibit colonic contractions in response to PACAP. Effects of PACAP are in addition to the previously described purinergic and sympathetic inputs to PIC. Thus, PIC integrate inhibitory inputs from at least 3 neurotransmitters and utilize several types of receptors to activate SK channels and regulate colonic contractile behaviors. (*Cell Mol Gastroenterol Hepatol* 2022;14:357-373; <https://doi.org/10.1016/j.jcmgh.2022.05.004>)

Keywords: Colon; Inhibitory Effects; Interstitial Cells; Peptidergic Neurotransduction.

Platelet-derived growth factor receptor α (PDGFR α)-positive interstitial cells (PIC) are interstitial cells interposed between enteric nerve fibers and smooth muscle cells (SMCs) in the tunica muscularis of the gastrointestinal (GI) tract. PIC, along with interstitial cells of Cajal (ICC), wrap around the varicose processes of enteric motor neurons that innervate the muscle layers along the length of GI tracts of mice and human.^{1,2} SMCs are electrically coupled to ICC and PIC via gap junctions, and the 3 types of cells operate together as a syncytium (referred to as the SIP syncytium), regulating the excitability and contractility of the GI musculature.³⁻⁵ PIC display robust expression of apamin-sensitive small conductance Ca²⁺ activated potassium channels 3 (SK3 channels), and, when activated, this conductance hyperpolarizes electrically coupled SMCs and causes inhibition of phasic contractions and relaxation.^{2,6-9} PIC have been reported to transduce inputs from enteric inhibitory motor neural signals by purinergic enteric neurons and sympathetic nervous system to membrane hyperpolarization by purinergic receptor P2Y1-SK channel signal pathway and α 1A adrenergic receptor-SK channel signal pathway, respectively.^{2,6-12} Deep sequencing of gene transcripts in small bowel and colonic PIC, purified by fluorescence-activated cell sorting (FACS), has shown that these cells also express a variety of receptors for additional neurotransmitters, hormones, and inflammatory mediators.¹³ Growing evidence suggests that PIC serve as a brake on GI motility, integrating inhibitory inputs from intrinsic and extrinsic nerves, hormones, and inflammatory mediators.

Pituitary adenylate cyclase-activating polypeptide (PACAP) is a 27- or 38-amino acid neuropeptide and a member of the secretin/glucagon/vasoactive intestinal polypeptide (VIP) family, discovered by Akira Arimura and his coworkers in 1989 as a hypothalamic polypeptide-stimulating adenylate cyclase in rat anterior pituitary cell cultures, as the name suggests.^{14,15} There are 3 G protein-coupled receptors (GPCR) for PACAP, PAC₁R, VPAC₁ receptor (VPAC₁R), and VPAC₂ receptor (VPAC₂R). The affinity of PAC₁R for PACAP is about 1000-fold higher than for VIP, and VPAC₁R and VPAC₂R exhibit similar affinities for PACAP and VIP.¹⁶⁻¹⁸ PACAP and its receptors are widely distributed in central nervous system and peripheral tissues and have a broad spectrum of physiological and pathophysiological roles.¹⁸ PACAP is expressed in the enteric nervous system, and the peptide hyperpolarizes GI muscles and inhibits contraction, which are effects that appear to be mediated by SK channels.¹⁸⁻²¹ From analysis of our transcriptome data, we noted that the major receptor for PACAP, PAC₁R, encoded by *Adcyap1r1*, is highly expressed in PIC in the colonic musculature (Figure 1, A)^{13,22,23} and, therefore, we hypothesized that PIC might transduce enteric inhibitory signals mediated by PACAP in the colon. The major mechanism typically considered for PAC₁R transduction, G_s-coupled activation of adenylate cyclase and formation of cAMP, would not be an appropriate signal for increasing intracellular Ca²⁺ concentration ([Ca²⁺]_i). However, some studies have also shown that PAC₁R can couple with G_{q/11} in cells,²⁴ providing a mechanism for activation of phospholipase C- β , enhanced

production of IP₃ and release of Ca²⁺ from intracellular stores via IP₃ receptors. Increasing [Ca²⁺]_i in PIC would provide a mechanism that could activate SK3 channels because these channels are Ca²⁺ activated. Thus, a mechanism equivalent to the activation of SK3 channels in PIC by purinergic and sympathetic nerve stimulation^{6,7,9} may be available for neurotransduction of PACAP. We investigated the responses of PIC to PACAP and a PAC₁R agonist and the effects of PIC activated by them on the colonic contractility in mouse and human colon.

Results


Adcyap1r1 is Expressed in PIC of Mouse Colon

Gene expression analysis was performed using quantitative polymerase chain reaction (qPCR) on RNA extracted from PIC, ICC, and SMCs isolated from colonic muscles and sorted to purity by FACS to confirm previous transcriptome data (Figure 1).^{13,22,23} These experiments confirmed that *Adcyap1r1* (encoding PAC₁R) is highly expressed in PIC and showed far lower expression in ICC and SMCs (Figure 1, B). *Vipr1* and *Vipr2* (encoding VPAC₁R and VPAC₂R, respectively) displayed low expression in PIC, ICC, and SMCs.

PACAP Elicited Ca²⁺ Transients in PIC of Mouse Distal Colon but not VIP

Ca²⁺ dynamics in PIC of the distal colon of PDGFR α -Cre-GCaMP6f mice and responses to PACAP were evaluated. Spindle-shaped cells and their responses to MRS2365 (P2Y1-specific agonist) were identified as PIC in the circular muscle (CM) layer of the colon, as previously described.⁹ Tetrodotoxin (TTX) (1 μ M) was added throughout the experiments to eliminate neuronal influences on the Ca²⁺ signaling in PIC. A combination of atropine (1 μ M) and N-Nitro-L-arginine methyl ester hydrochloride (L-NNA) (100 μ M) were also used to reduce contamination from cholinergic and nitroergic responses throughout the experiments. Under these control conditions, PIC fired discrete and localized Ca²⁺ transients, which occurred in 17.3% \pm 4% of cells at an average of 4.6 \pm 0.9 events/min (range, 2–8 events/min; n = 5). PACAP (100 nM; Figure 2, C–E) increased Ca²⁺ transients in PIC. The

Abbreviations used in this paper: AUC, area under the curve; [Ca²⁺]_i, intracellular Ca²⁺ concentration; CM, circular muscle; EFS, electrical field stimulation; FACS, fluorescence-activated cell sorting; GI, gastrointestinal; GPCR, G-protein coupled receptors; ICC, interstitial cells of Cajal; IP₃, inositol triphosphate; KRB, Krebs-Ringer bicarbonate solution; L-NNA, N-Nitro-L-arginine methyl ester hydrochloride; MXD, maxadilan; NE, norepinephrine; PACAP, pituitary adenylate-cyclase-activating polypeptide; PDGFR α , platelet-derived growth factor receptor α ; PE, phenylephrine; PIC, PDGFR α + interstitial cells; PSS, physiological salt solution; qPCR, quantitative polymerase chain reaction; SK channels, small conductance Ca²⁺-activated K⁺ channels; SMCs, smooth muscle cells; SPCs, spontaneous phasic contractions; STM, spatiotemporal maps; T1/2, half-times of the hyperpolarization responses; TTX, tetrodotoxin; VIP, vasoactive intestinal polypeptide.

 Most current article

© 2022 The Authors. Published by Elsevier Inc. on behalf of the AGA Institute. This is an open access article under the CC BY-NC-ND license (<http://creativecommons.org/licenses/by-nc-nd/4.0/>).

2352-345X

<https://doi.org/10.1016/j.jcmgh.2022.05.004>

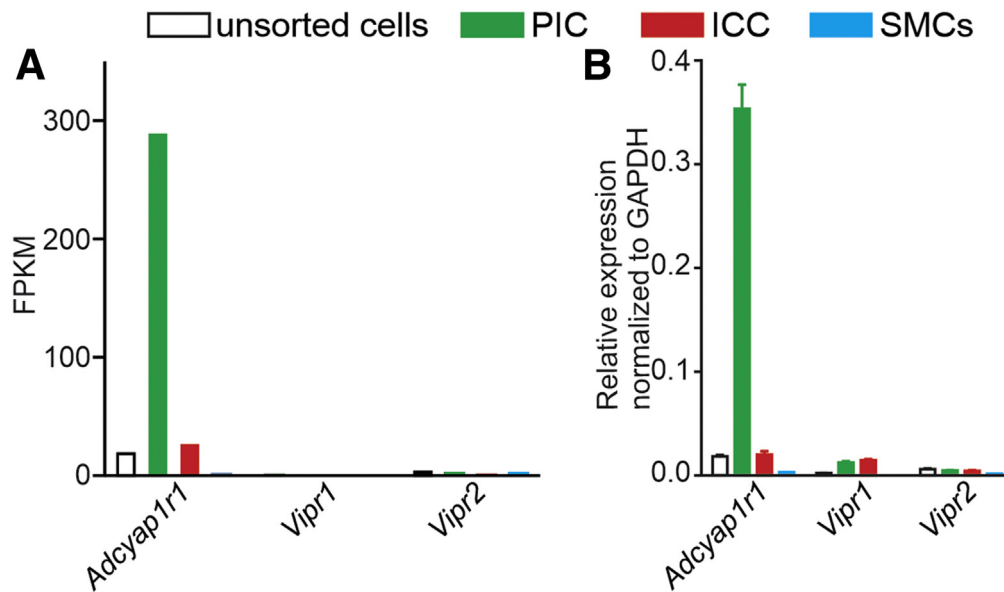


Figure 1. The expression of PAC₁R gene in SIP syncytium. A, The graph depicting the expression of the genes of PAC₁R (*Adcyap1r1*), VPAC₁R (*Vipr1*), and VPAC₂R (*Vipr2*) created from the transcriptome data of SIP syncytium of mouse colon that were published in 2015 to 2017.^{13,22,23} Fragments per kilobase of transcript per million (FPKM) of *Adcyap1r1*, *Vipr1*, and *Vipr2* are 290.71, 0.12, and 4.28 in PIC, 28.19, 0.12, and 1.04 in ICC, and 1.97, 0.00, and 4.19 in SMCs, respectively. B, The graph of the expression of *Adcyap1r1*, *Vipr1*, and *Vipr2* in each of cells in SIP syncytium analyzed by qPCR from 3 mouse colonic musculatures of each of SMC-eGFP, ICC-copGFP, and PDGFR α -eGFP mice. Bars and vertical lines represents means and standard deviation, respectively. As the transcriptome data, *Adcyap1r1* was predominantly expressed in PIC.

majority of these responses were initiated with high amplitude Ca²⁺ transients, which were followed by a sustained series of Ca²⁺ oscillations that tapered off gradually. PACAP significantly increased the frequency of Ca²⁺ transients in PIC from 4.6 ± 1.2 to 37.8 ± 3.9 per minute (Figure 2, F) ($P < .0001$; $n = 5$) and increased Ca²⁺ transient amplitude from 78.8 ± 8.9 to 141.4 ± 10.5 (Figure 2, G) ($P < .0019$; $n = 5$). The duration and spatial spread of Ca²⁺ transients did not change significantly (Figure 2, H–I) ($P < .8$ and $P < .4$, respectively; $n = 5$). Pre-treatment of colonic muscles with PAC₁R antagonist, PACAP 6-38 (1 μ M), had no effect on basal Ca²⁺ transients in PIC (frequency 4.6 ± 1.2 per minute), but it blocked the response to PACAP. Frequency (Figure 2, F) ($P < .13$), amplitude (Figure 2, G) ($P < .8$), duration (Figure 2, H) ($P < .9$), and spatial spread (Figure 2, I) ($P < .79$) of Ca²⁺ transient parameters were unchanged by PACAP in the presence of PACAP 6-38. Application of VIP 100 nM had no significant effects on PIC Ca²⁺ transients across all parameters (Figure 3).

PACAP Inhibited Spontaneous Phasic Contractions of Mouse Distal Colon Through SK Channels

The effects of activation of PICs by PACAP on spontaneous phasic contractions (SPCs) of CM of mouse distal colon were evaluated in contractile experiments (Figure 4). PACAP inhibited the amplitude of SPCs in a concentration-dependent manner (Figure 4, Aa; $n = 5$). Apamin (300 nM; $n = 6$) significantly reduced the inhibitory effects of PACAP on SPCs (Figure 4, Ab), indicating that the inhibitory effects were mediated by SK channels. Figure 4, B showed the summary

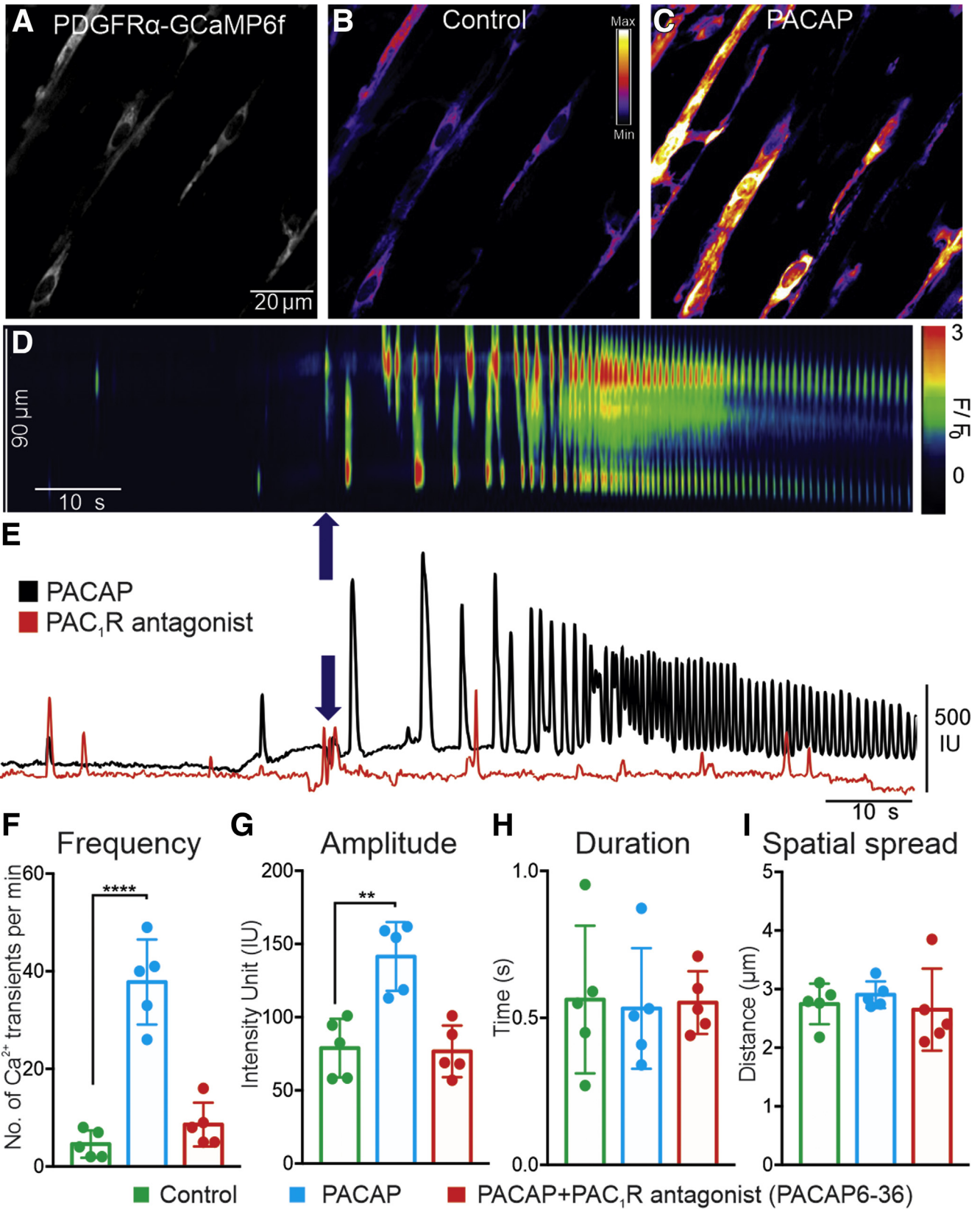
graphs of 4 parameters, area under the curve (AUC) (Figure 4, Ba), amplitude (Figure 4, Bb), tone (Figure 4, Bc), and frequency (Figure 4, Bd), of SPCs of CM of mouse distal colon. The values of those 4 parameters are shown in Table 1.

PACAP Elicited Ca²⁺ Transients in PIC of Human Sigmoid Colon

We evaluated Ca²⁺ signaling in PIC of human sigmoid colon in response to PACAP using a wide field imaging system. Based on the finding in our previous study,¹² PIC were identified as stellate-shaped cells at myenteric plexus that responded to electrical field stimulation (EFS: pulse width 50 μ s, 20 Hz, 1 s, supramaximal voltage) in a MRS2500 (selective P2Y1 purinoceptor antagonist)-sensitive manner (Figure 5, A–C) or with increased Ca²⁺ responses to phenylephrine (PE) 10 μ M (21 cells; $n = 3$). Thus, EFS or PE (10 μ M) accelerated and enlarged spontaneous Ca²⁺ transients in PIC or induced either sustained or oscillatory increases in basal Ca²⁺ levels. PACAP (100 nM) enhanced spontaneous Ca²⁺ transients or developed a transient rise in the basal Ca²⁺ level in those PIC with a variable latency (Figure 5, D) (14 cells; $n = 3$).

Maxadilan Hyperpolarizes SMCs Through SK Channels

In the next series of experiments, we tested the effects of maxadilan (MXD), a selective PAC₁R agonist, on membrane potentials of human colonic muscles using intracellular electrical recording. Human S colon CM cells had resting membrane potentials averaging -46 ± 1.2 mV ($n = 10$).



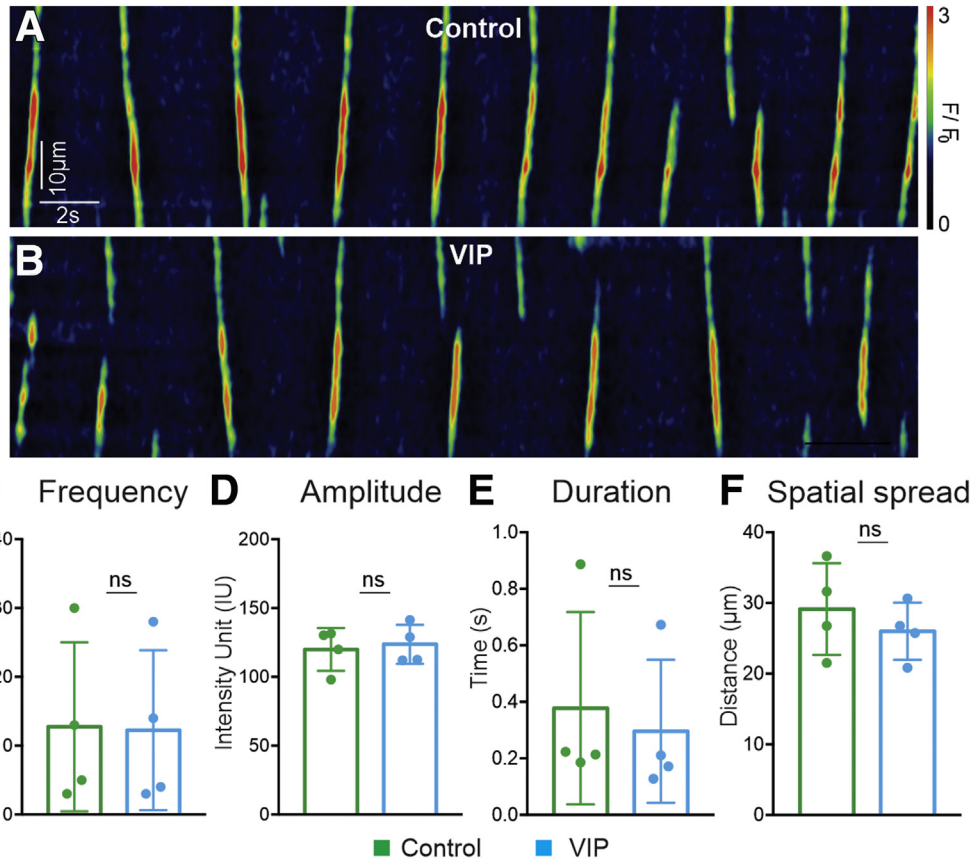


Figure 3. Ca²⁺ responses of PICs to VIP in mouse distal colon. *A* and *B*, Spatiotemporal Ca²⁺ map (STMap) showing Ca²⁺ transient firing patterns in PIC under control conditions (*A*) and in the presence of VIP 100 nM (*B*). Summary of Ca²⁺ transient parameters are shown: frequency (*C*); Ca²⁺ transient amplitude (*D*); Duration (*E*); and Spatial spread (*F*) ($n = 4$ for each of control and VIP groups). In all graphs, boxes, dots, and vertical lines represent means, individual values, and standard deviation, respectively. ns denotes no significant difference between control and after VIP application.

MXD (10 nM) evoked slow hyperpolarization of -9.8 ± 1.5 mV ($n = 4$) (Figure 6, *Aa*, left panel). Apamin (100 nM) depolarized cells by 1.9 ± 0.5 mV ($n = 4$) and inhibited hyperpolarization responses to MXD ($n = 4$) (Figure 6, *Aa*, right panel), indicating that the responses to MXD were caused by opening of SK channels.

To characterize the responses of human colonic muscles to PAC₁R agonist, we compared it with the responses to P2Y₁ receptor agonist MRS2365 and norepinephrine (NE). MRS2365 (100 nM) and NE (10 μM) also hyperpolarized human colonic muscles via activation of SK channels in PIC (MRS2365, -9.1 ± 1.2 mV, $n = 6$; NE, -16.3 ± 1.7 mV, $n = 4$) (Figure 6, *Ba* right panel), as previous described,¹² but the hyperpolarization induced by MXD (10 nM) reached the maximum hyperpolarized level much more slowly than the responses to MRS2365 or NE (Figure 6, *Ba*, right panel). To assess the time course of hyperpolarization induced

by the 3 drugs, the half-times of the hyperpolarization responses ($T_{1/2}$) were measured as illustrated in Figure 6, *Ba*. Figure 6, *Bb* shows that $T_{1/2}$ for responses induced by MXD was significantly longer than responses induced by MRS2365 or NE.

PACAP and MXD Inhibited SPCs of Human Sigmoid Colon Through SK Channels

Contractile experiments were performed to test the effects of PACAP and PAC₁R agonist MXD on SPCs of CM of human sigmoid colon (Figure 7 and 8). These experiments were conducted in the presence of TTX. PACAP and MXD inhibited the amplitude of SPCs in a concentration-dependent manner (Figure 7, *Aa* and 8, *Aa*; $n = 6$). Apamin (100 nM; $n = 6$) significantly reduced the inhibitory effects of PACAP and MXD on SPCs (Figure 7, *Ab* and 8, *Ab*),

Figure 2. (See previous page). Ca²⁺ responses of PIC to PACAP in mouse distal colon. *A*, Representative raw image of PIC in the intramuscular region of the distal colon taken from PDGFR α -Cre-GCaMP6f mice. *B*, A purple hue was added as an overlay to enhance visualization; color scale indicates intensity of Ca²⁺ transients (ie, dark blue is low fluorescence; light yellow to white indicates high fluorescence levels). *C*, Image showing Ca²⁺ responses of PIC in response to PACAP (100 nM) application. Scale bar in *A* is 20 μm and pertains to all images. *D*, Spatio-temporal Ca²⁺ map (STMap) showing Ca²⁺ transient firing patterns in PIC in response to PACAP. The arrow (blue) in *D* indicates PACAP application. *E*, Representative traces of Ca²⁺ transients in PICs elicited by PACAP (100 nM, in black) and in the presence of PAC₁R antagonist PACAP 6-38 (1 μM, in red). The arrow (blue) in *E* indicates PACAP application point ($n = 5$). Summary of Ca²⁺ transient parameters are shown: Frequency (*F*); Ca²⁺ transient amplitude (*G*); duration (*H*); and spatial spread (*I*) ($n = 5$ for each of Control, PACAP, and PACAP+PAC₁R antagonist). In all graphs, boxes, dots, and vertical lines represent means, individual values, and standard deviation, respectively. *Denotes significant difference between control and after PACAP application. **.01 > $P \geq .001$; **** $P < .0001$.

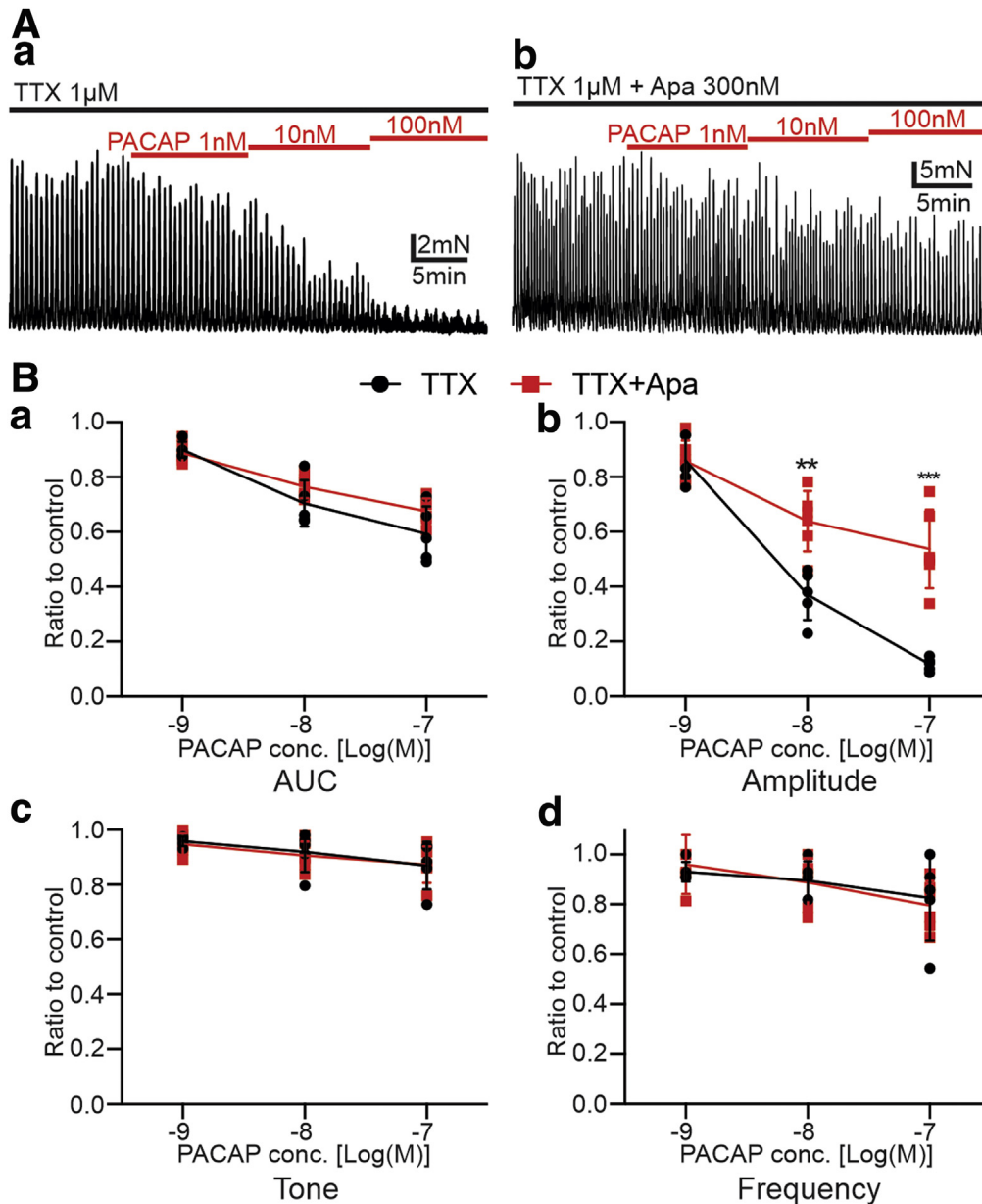


Figure 4. The responses of SPCs of mouse distal colonic circular muscle to PACAP. **A**, PACAP inhibited SPCs in a concentration-dependent manner (*Aa*; $n = 5$). Apamin (Apa; 300 nM) inhibited the effects of PACAP (*Ab*; $n = 6$). **B**, Summaries of 4 contractile parameters, AUC (*Ba*), amplitude (*Bb*), tone (*Bc*), and frequency (*Bd*), were tabulated as the ratio of SPCs after administration of PACAP to before administration of PACAP (control) (TTX; $n = 5$; TTX + Apa; $n = 6$). In all graphs, diagonal lines, dots, and vertical lines represent means, individual values, and standard deviation, respectively. *Denotes significant difference of the ratios between with and without apamin. *.05 > $P \geq .01$; **.01 > $P \geq .001$; ***.001 > $P \geq .0001$; ****.0001 > P .

indicating that the inhibitory effects of PACAP and MXD were mediated by SK channels. Figures 7, B and 8, B show summary data for the effects of PACAP and MXD and these drugs in the presence of apamin for AUC (Figures 7, Ba and 8, Ba), amplitude (Figures 7, Bb and 8, Bb), tone (Figures 7, Bc and 8, Bc), and frequency (Figures 7, Bd and 8, Bd) of SPCs of CM of human sigmoid colon. The values of those 4 parameters are shown in Table 2 and 3.

Latency of the Response of SPCs of CM of Human Sigmoid Colon to PAC₁R Agonists

Latency of responses to PACAP and MXD on SPCs were compared with responses to NE with propranolol (to favor stimulation of α_1 adrenoceptor) to further characterize the responses of human colonic muscles to the PAC₁R agonist.

The duration between administration of the minimum concentrations capable of maximum inhibition of SPCs and the time when cessation of SPCs occurred (latency) were measured for responses to NE (Figure 9, Aa; $n = 10$), PACAP (Figure 9, Ab; $n = 6$) and MXD (Figure 9, Ac; $n = 6$). Latencies of PACAP and MXD were significantly longer than that of NE (Figure 9, B).

Discussion

Interstitial cells different from ICC have been reported in the smooth muscle tissues of the GI tract since the 1980s. These unique interstitial cells were called 'fibroblast-like cells' because of their ultrastructural features.^{3,25,26} In 2009, lino et al reported that the fibroblast-like cells expressed PDGFR α as a cell-specific marker and, therefore, these cells

Table 1. Tables Summarizing Means \pm SD of 4 Parameters of Spontaneous Contractions of Circular Muscle Layers of Mouse Distal Colon for 5 Minutes After Adding PACAP 1 nM to 100 nM to Organ Baths

	AUC, mN·min		
	1 nM	10 nM	100 nM
TTX (5) ^a	45.63 \pm 5.85	35.73 \pm 6.53	30.07 \pm 6.61
TTX + Apa (6)	49.97 \pm 8.17	43.14 \pm 7.52	37.94 \pm 6.03
	Amplitude, mN		
	1 nM	10 nM	100 nM
TTX (5)	10.26 \pm 2.49	4.32 \pm 1.17	1.36 \pm 0.23
TTX + Apa (6)	16.40 \pm 5.11	12.58 \pm 5.65	10.77 \pm 5.85
	Tone, mN		
	1 nM	10 nM	100 nM
TTX (5)	6.06 \pm 1.40	5.82 \pm 1.45	5.50 \pm 1.37
TTX + Apa (6)	6.07 \pm 1.39	5.80 \pm 1.34	5.60 \pm 1.37
	Frequency, cont/min		
	1 nM	10 nM	100 nM
TTX (5)	2.12 \pm 0.27	2.04 \pm 0.33	1.88 \pm 0.44
TTX + Apa (6)	2.87 \pm 0.69	2.63 \pm 0.46	2.33 \pm 0.21

Apa, Apamin; AUC, area under the curve; PACAP, pituitary adenylate-cyclase-activating polypeptide; SD, standard deviation; TTX, tetrodotoxin; WT, wild type.

In amplitude, 2 groups had significant differences at PACAP 10 nM ($P = .0019$) and 100 nM ($P = .0001$).

^aNumbers in parentheses represent the number of mice in each of the protocols.

began to be known as PDGFR α^+ cells.¹ We reported that PDGFR α^+ cells exist in human colon in the same anatomical niches as in mouse colon, exhibit robust expression of SK3 channels, and are the effector cells, in which P2Y1 receptor binding activates SK channels in PDGFR α^+ cells, the hallmark of the purinergic component of enteric inhibitory signaling, and, also, α 1A adrenoceptor (α 1A AR) binding activates SK channels in PDGFR α^+ cells, mediating sympathetic inhibitory inputs in mouse and human colon.^{2,6,7,9,12} PDGFR α^+ cells have been reported to exist in the lamina propria of GI mucosa,²⁷ and, therefore, we suggested referring to them as PDGFR α^+ interstitial cells (PIC) to distinguish them from the other types of cells that express PDGFR α .

Nerve fibers with PACAP-like immunoreactivity have been reported in GI tract and located in myenteric plexus, submucosal plexus, some enteric neurons' nerve processes in the circular and longitudinal muscle layers of rat, guinea pig, and human.²⁸⁻³⁰ PIC are in close contact with enteric ganglia and nerve bundles, forming a mesh-like network in all layers (ie, plane of the myenteric plexus and circular and longitudinal muscle layers) of mouse and human colon.^{1,2,6} Thus, it is likely that PACAP released from enteric motor neurons binds to receptors expressed by PIC.

Experiments on mouse colon in this study confirmed that *Adcyap1r1* is highly expressed by PIC in the SIP syncytium,

and far lower levels of expression were detected in SMCs and ICC (Figure 1). It is also interesting that expression of *Vipr1* and *Vipr2* were very low in SIP cells, although resolvable expression was detected in PIC and ICC. These results suggest that PIC could be the major cells in which PACAP neurotransduction occurs. Serio et al reported that PACAP caused hyperpolarization of CM in mouse distal colon by a mechanism similar to adenosine 5' triphosphate, as responses to both agonists were inhibited by apamin.²⁰ These findings suggest the involvement of SK channels in transduction of both adenosine 5' triphosphate and PACAP, and our experiments showed that Ca²⁺ transients were increased in PIC in response to PACAP (Figure 2). Increasing Ca²⁺ transients by PACAP is an appropriate signal for increasing the open probability of SK channels, because these channels are activated by [Ca²⁺]_i. Contractions of CM from mouse distal colons were inhibited by PACAP, and these responses were blocked by apamin, an SK channel antagonist (Figure 4). SK channels (ie, SK3) are expressed predominantly in PIC.^{6,9,13,31} Taken together, our data show that the primary receptor for PACAP, PAC₁R, is highly expressed in PIC, and PACAP binding to this receptor activates Ca²⁺ transients that would be expected to activate SK3 channels in PIC. Utilizing this pathway, PACAP inhibits colonic contractions, and these responses are sensitive to block by apamin. Thus, our data are consistent with PIC being a primary post-junctional target for PACAP neurotransmission in mouse colon. The limitation of our

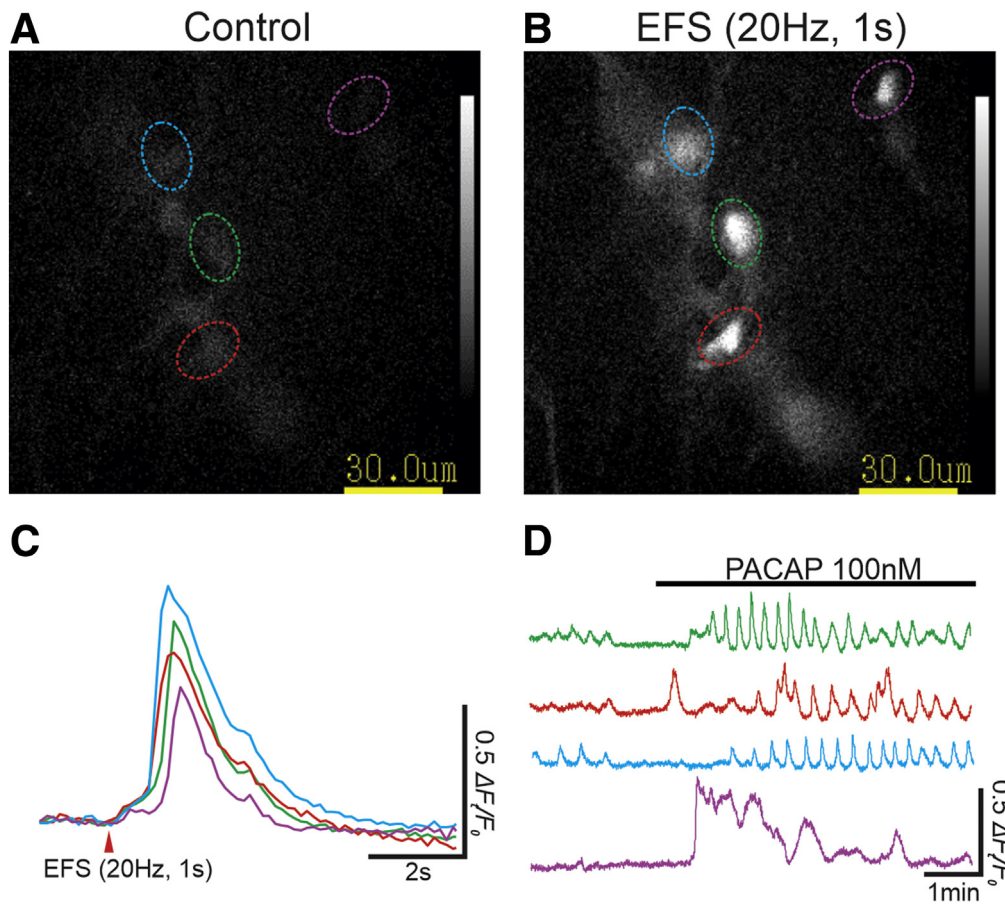


Figure 5. Ca^{2+} responses of PIC to PACAP in human sigmoid colon. *A* and *B*, Four PIC (dot circles in blue, pink, green, and red) in the myenteric plexus of a longitudinal layer preparation of human sigmoid colon responded to EFS (pulse width $50\mu\text{s}$, 20Hz, 1s, supramaximal voltage) by generating Ca^{2+} transients (*A* and *B*). *C*, Graph C depicts the EFS-induced responses of the PIC in *A* where each trace color is corresponding to the color of the dot circles in *A*. These responses were abolished by MRS2500 $1\mu\text{M}$, a P2Y1 purinoceptor antagonist, indicating that these cells are PIC (21 cells; $n = 3$).¹² *D*, In the same preparation, bath applied PACAP (100 nM) facilitated spontaneous Ca^{2+} transients or developed a transient raise in the basal Ca^{2+} level in the PIC (14 cells; $n = 3$). Each trace color is corresponding to the color of the dot circle in *A* or the trace in *C*.

study is not to have used PIC-specific knock-out mice of PAC₁R or SK3 channels, which would provide more definitive evidence of the roles of these cells in PACAP signaling for colonic motility. Further studies are required.

We also found that PACAP induced or enhanced Ca^{2+} transients in PIC in human colon. PIC were identified in human muscles by their signature responses to phenylephrine or MRS2500-sensitive responses to electrical nerve stimulation (Figure 5).¹² Membrane potential recordings from CM of human sigmoid colon demonstrated that PAC₁R agonist MXD evoked the hyperpolarization, which was inhibited significantly by apamin (Figure 6). These data suggest that the rise of Ca^{2+} in PIC in response to binding of PACAP receptors triggers the opening of SK channels and the development of hyperpolarization. These responses can be conducted to SMCs due to the gap junction coupling between SMCs and PIC.³ Contractile experiments showed that SPCs of colonic muscles were inhibited significantly by PACAP or MXD, and the inhibitory responses were reduced by apamin (Figures 7 and 8). SK3 channels are the dominant subtype of SK channels in human colon (nTPM of SK1, SK2, and SK3 are 0.3, 0.9, and 5.6, respectively) (www.proteinatlas.org),³² and SK3 channels are expressed predominantly in human PIC.² These data suggest that a PAC₁R-SK channel signal pathway is also available in human colonic

muscles, and, as in mice, PIC are post-junctional targets for PACAP transmission. A schematic diagram of PACAP signaling, as supported by the results of this study, is depicted in Figure 10.

Responses of mouse PIC and human PIC to PACAP were similar, but not identical, in this study. In human contractile experiments, the latency of the responses to PACAP and MXD were significantly longer than NE with propranolol (stimulation of $\alpha 1$ adrenoceptor) (Figure 9). However, in mouse colon, the difference of the latency of responses to PACAP and phenylephrine are not significant (Figure 4).⁹ This can also be seen in the electrophysiological responses induced by MXD that were significantly slower to develop than responses to NE and MRS2365, a selective P2Y1 receptor agonist (Figure 6, B). The receptors for responses in PIC to NE and MRS2365 are $\alpha 1A$ AR and P2Y1 receptor, respectively, which are GPCRs,^{9,12} and both of these receptors are coupled through $G_{q/11}$.^{33,34} PAC₁R displays mixed coupling through both G_s and $G_{q/11}$, the characteristics of which vary depending upon the splice variants expressed.²⁴ It has been reported that GPCR coupled through G_s reduces $[\text{Ca}^{2+}]_i$ and inhibits signaling of GPCR through $G_{q/11}$.^{35,36} Therefore, the slower and delayed responses of PIC in human colon and the difference of the responses of mouse and human PIC to PAC₁R agonists might

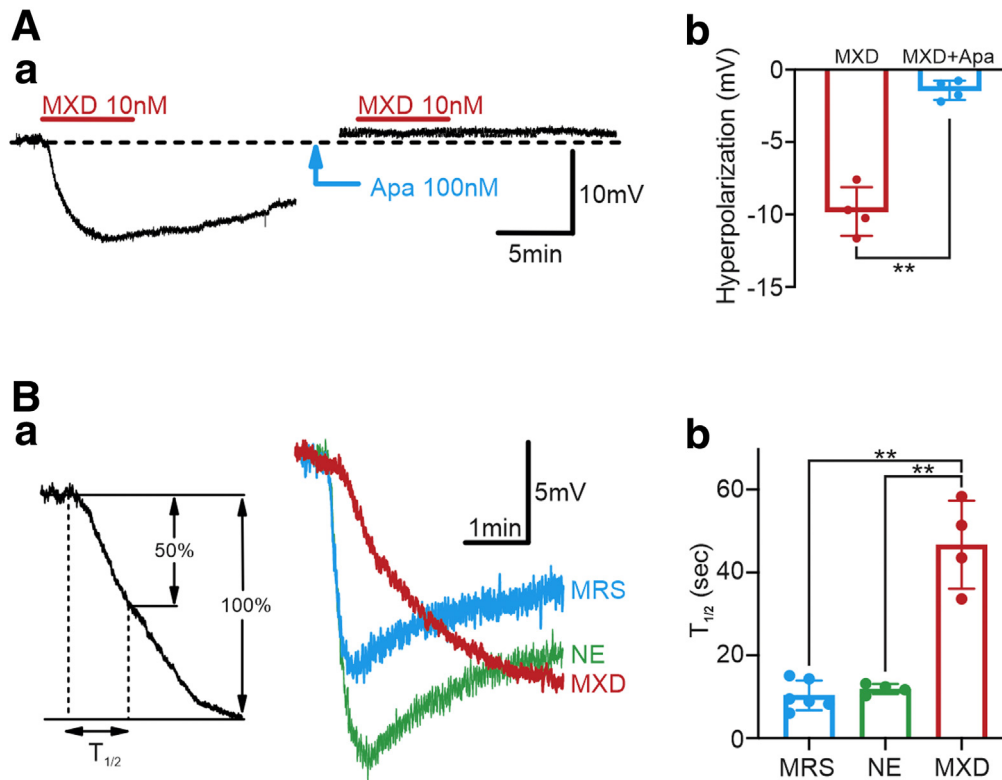


Figure 6. The effects of MXD on membrane potentials of human sigmoid colonic circular smooth muscle cells. **A**, MXD-induced hyperpolarization was inhibited by pretreatment of Apamin (Apa) 0.1 μ M ($n = 4$). Two traces were recorded from the same impalement with a resting membrane potential of -44 mV (**Aa**). **Ab** depicts summarized graphs showing the effects of Apa on MXD-induced hyperpolarization (**Ab**; $n = 4$). ****P** < .01, significant difference from control responses. **B**, The half-hyperpolarizing time ($T_{1/2}$) was measured as the mean time taken for 50% hyperpolarization in the amplitude of the peak hyperpolarization (**Ba**, left panel). **Ba**, right panel depicts high-speed traces of hyperpolarization produced by MRS2365 (100 nM), norepinephrine (NE; 10 μ M), and MXD (10 nM). **Bb** depicts summarized graphs showing $T_{1/2}$ (sec) calculated from the hyperpolarization induced by MRS2365 (100 nM) ($n = 6$), NE (10 μ M) ($n = 4$), and MXD (10 nM) ($n = 4$). $T_{1/2}$ of the response to MXD was significantly longer than the ones to MRS2365 and NE. ****P** < .01, significant difference from MRS2365 and NE. In all graphs, boxes, dots, and vertical lines represent means, individual values, and standard deviation, respectively.

be attributed to relative influences of coupling via G_s vs $G_{q/11}$ or to the balance of expression of $VPAC_1R$ or $VPAC_2R$ in human PIC. Further study will be required to address these questions.

PACAP and VIP are inhibitory peptidergic neurotransmitters with different signaling pathways in GI muscles.^{19,37,38} In the gene expression analysis performed in this study, *Vipr1* and *Vipr2*, as well as *Adcyap1r1*, were expressed in cells of the SIP syncytium in the mouse but *Vipr1* and *Vipr2* transcripts were expressed at much lower level than *Adcyap1r1*. $VPAC_1R$ and $VPAC_2R$ are coupled with G_s ³⁹ and, therefore, VIP has been presumed to inhibit contractions of colonic muscles by activating K^+ channels via cAMP signaling pathway^{19,37,38} or by reducing $[Ca^{2+}]_i$ and inhibiting the signaling of GPCR through $G_{q/11}$, as described above. If the latter mechanism is important, VIP is likely to use ICCs or SMCs as effector cells, but not PIC. This is because reducing $[Ca^{2+}]_i$ in PIC would inhibit openings of SK channels and reduce the inhibitory drive on the SIP syncytium, which in essence would be an excitatory influence rather than inhibitory

drive on SMCs. In this study, VIP 100 nM did not significantly affect Ca^{2+} transients in PIC (Figure 3). Therefore, it seems likely that PACAP and VIP utilize different effector cells to exert inhibitory effects on colonic muscle contractions.

PACAP is reported to be released under stressful conditions and cause catecholamine secretion from chromaffin cells.⁴⁰ In our recent human tissue study,¹² we found that the effects of catecholamine on PIC desensitized as a function of time and SPCs came back within 20 minutes after administration of NE 10 μ M in the presence of TTX 1 μ M and propranolol 1 μ M in 11 of 11 cases (100%), whereas in this study, the effects of PAC_1R agonists were more persistent, and SPCs came back within 20 minutes after administration of PACAP 100 nM or MXD 10 nM in only 1 of 11 cases (9%) in human study. The slower and prolonged inhibitory effects of PAC_1R agonists on colonic contractility might be a means of compensating for the brevity of catecholamine effects during sustained stress. Additionally, we did not detect any differences between males and females in the effects of NE and PACAP on mouse and human colon,

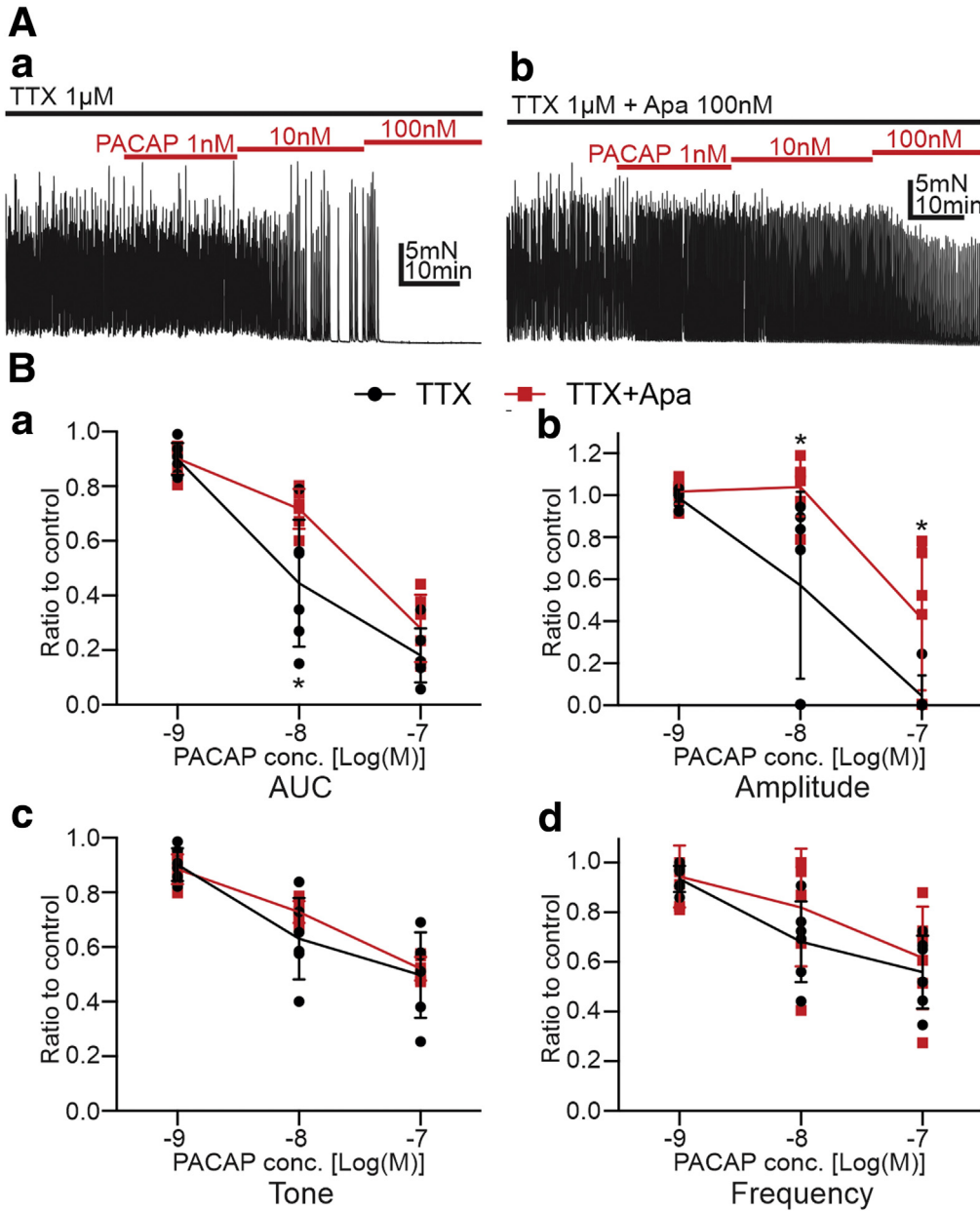


Figure 7. The responses of SPCs of human sigmoid colonic muscle to PACAP. **A**, PACAP inhibited SPCs in a concentration-dependent manner (*Aa*; $n = 6$). Apamin (Apa; 100 nM) inhibited the effects of PACAP (*Ab*; $n = 6$). **B**, Summaries of 4 contractile parameters, AUC (*Ba*), amplitude (*Bb*), tone (*Bc*), and frequency (*Bd*), were tabulated as the ratio of SPCs after administration of PACAP to before administration of PACAP (control). In all graphs, diagonal lines, dots, and vertical lines represent means, individual values, and standard deviation, respectively. *Denotes significant difference of the ratios between with and without apamin ($P < .05$).

which suggests that the stress might be able to cause the inhibition of colonic motility by NE and PACAP equally for both genders.

In conclusion, the present study demonstrates that PIC in mouse and human colon express and utilize a PAC₁R-SK channel signal pathway to mediate inhibitory regulation of colonic contractile activity by PACAP. PIC also have receptors for purines (P2Y1) and catecholamines (α 1A AR), suggesting that these cells receive and integrate inhibitory neural signals to the SIP syncytium and provide important inhibitory regulation of colonic motility. Further investigation of functional roles of PIC in physiology and pathophysiology of colonic motility might lead to the development of new treatments for functional bowel disorders.

Methods

Animals

B6.129S4-Pdgfra^{tm11(EGFP)Sor}/J heterozygote mice (PDGFR α -eGFP mice), which express enhanced green fluorescent protein (eGFP) in nuclei of PDGFR α expressing cells throughout the body (Hamilton 2003),⁴¹ their wild-type siblings (C57BL/6), C57BL/6-Tg(Pdgfra-cre)1Clc/J (PDGFR α -Cre mice), B6.Cg-Tg(Myh11-cre,-EGFP)2Mik/J (SMC-eGFP mice), and B6;129S-Gt(ROSA)26Sor^{tm95.1(CAG-GCaMP6f)Hze}/J (GCaMP6 mice) were obtained from Jackson Laboratory (Bar Harbor, ME). The PDGFR α -Cre-GCaMP6f mouse strain was developed by crossing PDGFR α -Cre mice and GCaMP6 mice. Kit^{+/copGFP} mice (ICC-copGFP mice) was previously generated in University of Nevada.⁴² Animals (6–12 weeks post-partum) were

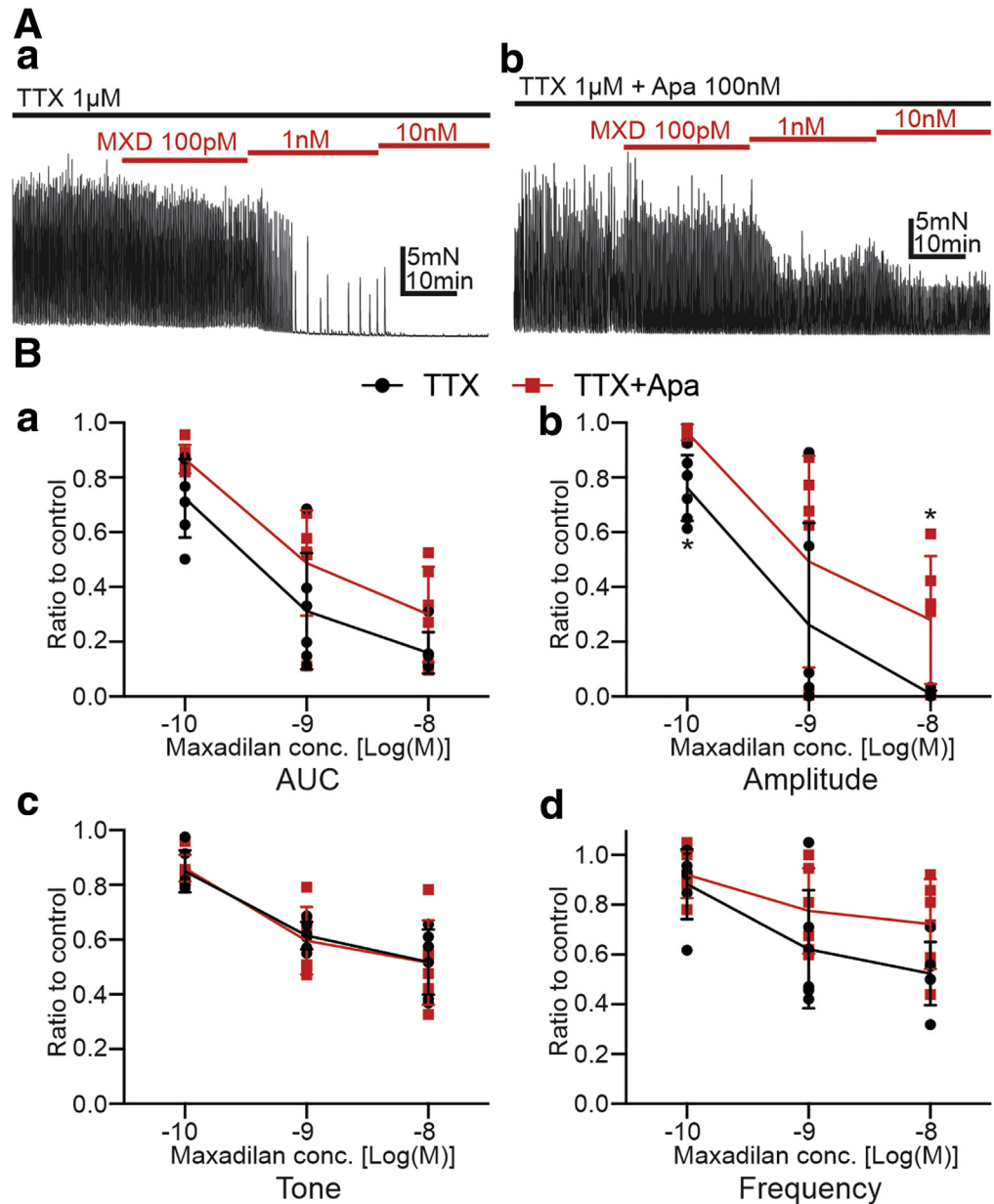


Figure 8. The responses of SPCs of human sigmoid colonic circular muscle to MXD. *A*, MXD inhibited SPCs in a concentration-dependent manner (*Aa*; $n = 6$). Apamin (Apa; 100 nM) inhibited the effects of MXD (*Ab*; $n = 6$). *B*, Summaries of 4 contractile parameters, AUC (*Ba*), amplitude (*Bb*), tone (*Bc*), and frequency (*Bd*), were tabulated as the ratio of SPCs after administration of PACAP to before administration of PACAP (control). In all graphs, diagonal lines, dots, and vertical lines represent means, individual values, and standard deviation, respectively. *Denotes significant difference of the ratios between with and without apamin ($P < .05$).

anesthetized by isoflurane (AErrane; Baxter, Deerfield, IL) and killed by cervical dislocation. The abdomens were opened, and colons were removed and used for experiments. Mice were maintained and the experiments performed in accordance with the National Institutes of Health Guide for the Care and Use of Laboratory Animals and the Institutional Animal Use and Care Committee at the University of Nevada, Reno, NV, approved experimental protocols.

Human Tissue

Human tissue samples were obtained from surgical waste of total 58 patients (34 males aged 50–83 years and 24 females aged 35–90 years) who underwent colectomy for colorectal cancer at the Department of Gastroenterological Surgery,

Nagoya City University from 2016 to 2017. All subjects were given written informed consent. The tumor-free parts of the human colorectum were used for experiments. The study design was approved by the Institutional Review Board of Nagoya City University. All samples were de-identified.

Analysis of Gene Expressions in PIC

SMC-eGFP, ICC-copGFP, and PDGFR α -eGFP mice colonic muscles were equilibrated in Ca $^{2+}$ -free Hank's solution, and cells were dispersed as described previously.⁴³

Fluorescence-activated cell sorting. GFP $^{+}$ cells were sorted by FACS with a Becton Dickinson FACSaria IITM instrument using a blue laser (488 nm) and the GFP/FITC emission detector (530/30 nm BP and 505 nm LP). Sorting was performed using a 130 μ m nozzle at a sheath pressure

Table 2. Tables Summarizing Means \pm SD of 4 Parameters of Spontaneous Contractions of Circular Muscle Layers of Human Sigmoid Colon for 10 Minutes After Adding PACAP 1 nM to 100 nM to Organ Baths

	AUC, mN·min		
	1 nM	10 nM	100 nM
TTX (6) ^a	73.56 \pm 19.25	39.09 \pm 27.01	15.31 \pm 10.95
TTX + Apa (6)	58.06 \pm 22.96	46.65 \pm 20.77	19.18 \pm 13.31
	Amplitude, mN		
	1 nM	10 nM	100 nM
TTX (6)	15.57 \pm 4.72	8.94 \pm 6.92	0.74 \pm 1.69
TTX + Apa (6)	15.65 \pm 5.19	16.11 \pm 6.14	6.85 \pm 5.90
	Tone, mN		
	1 nM	10 nM	100 nM
TTX (6)	2.37 \pm 1.03	1.70 \pm 0.94	1.32 \pm 0.73
TTX + Apa (6)	1.32 \pm 0.53	1.09 \pm 0.44	0.78 \pm 0.32
	Frequency, cont/min		
	1 nM	10 nM	100 nM
TTX (6)	3.92 \pm 0.80	2.80 \pm 0.66	2.28 \pm 0.52
TTX + Apa (6)	3.03 \pm 0.87	2.57 \pm 0.84	1.90 \pm 0.61

Apa, Apamin; AUC, area under the curve; PACAP, pituitary adenylate-cyclase-activating polypeptide; SD, standard deviation; TTX, tetrodotoxin; WT, wild type.

In amplitude, 2 groups had significant differences at PACAP 10 nM ($P = .03$) and 100 nM ($P = .04$). In AUC, 2 groups had significant differences at PACAP 10 nM ($P = .01$).

^aNumbers in parentheses represent the number of mice in each of the protocols.

of 12 psi and sort rate of 1000 to 3000 events per second. Live cells gated on exclusion of Hoechst 33258 viability indicator dye (data not shown) were subsequently gated on GFP fluorescence intensity.

Isolation of total RNA and qPCR. Total RNA was isolated from sorted GFP⁺ cells and unsorted cells using illustra RNAspin Mini RNA Isolation kit (GE Healthcare, Little Chalfont, UK). Concentration and purity of RNA were checked using an ND-1000 Nanodrop Spectrophotometer (Nanodrop, Wilmington, DE), comparative amount of RNA was used for first-strand cDNA synthesized with SuperScript III (Invitrogen, Carlsbad, CA), according to the manufacturer's instructions. qPCR was performed with specific primers (Table 4) using Fast Sybr green chemistry (Applied Biosystems, Foster City, CA) on the 7900HT Real Time PCR System (Applied Biosystems).

Ca²⁺ Imaging in Mice

Isolated distal colons (1.5–2.0 cm), 1.5 cm rostral to the anus, were removed and placed in a Krebs-Ringer bicarbonate solution (KRB) and opened along the mesenteric border. Inside contents were cleared and the mucosal layers were removed by sharp dissection. Tissues were isolated and pinned to the base of a Sylgard-coated dish with the serosal aspect of the colon facing down. The preparation was continuously

perfused with the KRB solution at 37°C for an equilibration period of 1 hour. Preparations were then visualized and imaged using a spinning-disk confocal microscope (CSU-W1 spinning disk; Yokogawa Electric Corporation, Tokyo, Japan) mounted to an upright Eclipse FN1 microscope equipped with 40 \times 0.8 NA and 60 \times 1.0 NA CFI Fluor lens (Nikon Instruments Inc, Melville, NY) with a continuous KRB perfusion of approximately 2 mL per minute as previously described.^{8,44} The GCaMP6f Ca²⁺ indicator expressed in PICs was excited at 488 nm using a laser coupled to a Borealis system (ANDOR Technology, Belfast, UK) to increase laser intensity and uniformity. The fluorescence emission (>515 nm) was captured using a high-speed EMCCD Camera (Andor iXon Ultra; ANDOR Technology). Experiments were performed in the presence of TTX, atropine, and L-NNA to exclude effects from neurogenic, cholinergic and nitrenergic pathways.

Ca²⁺ event analysis. All image sequences and movies of Ca²⁺ activity was collected at 33 fps using MetaMorph (Molecular Devices, San Jose, CA) as previously described.^{8,44} Movies were converted to stacked TIFF (tagged image file format) images and image processing and analysis was done using a custom software (Volumetry G8a, G.W.H.). Tissue movement was stabilized to ensure accurate measurements of Ca²⁺ transients from identified cells and background subtraction was applied to movies to better enhance the dynamic contrast of Ca²⁺ transients shown in

Table 3. Tables Summarizing Means \pm SD of 4 Parameters of Spontaneous Contractions of Circular Muscle Layers of Human Sigmoid Colon for 10 Minutes After Adding MXD 100 pM to 10 nM to Organ Baths

	AUC, mN·min		
	100 pM	1 nM	10 nM
TTX (6) ^a	43.62 \pm 25.67	18.69 \pm 17.02	8.10 \pm 3.59
TTX + Apa (6)	59.20 \pm 19.63	36.11 \pm 17.72	22.71 \pm 15.67
	Amplitude, mN		
	100 pM	1 nM	10 nM
TTX (6)	8.81 \pm 4.16	2.74 \pm 4.09	0.07 \pm 0.05
TTX + Apa (6)	13.13 \pm 4.20	7.63 \pm 6.05	4.21 \pm 3.29
	Tone, mN		
	100 pM	1 nM	10 nM
TTX (6)	1.38 \pm 0.75	0.97 \pm 0.46	0.78 \pm 0.35
TTX + Apa (6)	1.49 \pm 0.75	1.04 \pm 0.53	0.90 \pm 0.50
	Frequency, cont/min		
	100 pM	1 nM	10 nM
TTX (6)	4.00 \pm 1.15	2.82 \pm 1.22	2.28 \pm 0.50
TTX + Apa (6)	3.80 \pm 0.58	3.15 \pm 0.48	2.95 \pm 0.69

Apa, Apamin; AUC, area under the curve; MXD, maxadilan, pituitary adenylate-cyclase-activating polypeptide; SD, standard deviation; TTX, tetrodotoxin; WT, wild type.

In amplitude, 2 groups had significant differences at MDX 100 pM ($P = .01$) and 10 nM ($P = .04$).

^aNumbers in parentheses represent the number of mice in each of the protocols.

PIC. Single whole-cell ROIs were used to generate spatio-temporal maps (STMaps) of Ca^{2+} activity in PICs recorded in situ. STMaps were then imported as TIFF files into Image J (version 1.40, National Institutes of Health, MD, USA, <http://rsbweb.nih.gov/ij>) for post hoc quantification analysis of Ca^{2+} events. The STMapAuto plugin was utilized for uniform STMap quantification, as described previously.⁴⁵

Mechanical Tension Recordings of Circular Muscle Strips of Mouse Distal Colon

Distal colon was dissected from wild-type mice, and the mucosa was peeled off. Threads were tied at both end of the strips of it, and contractions of circular muscle layer were measured using an isometric force transducer (model TST105A; Biopac Systems Inc, Santa Barbara, CA) and the Biopac Acqknowledge software (Biopac Systems Inc). The muscle strips were perfused with oxygenated, warmed (36°C) Krebs solution for 1 hour, and then the muscles were stretched (20–30 mN). The experimental protocols were started when the SPCs and basal tension became consistent, about 1 hour after applying the initial stretch. Each of the experimental protocols was applied to one sample, and any multiple experimental protocols were not applied in one single samples. To analyze the responses of SPCs to PACAP in the specific conditions, 4 parameters of SPCs (AUC, amplitude, tone, and frequency) were measured for 5

minutes after adding PACAP 1 nM to 100 nM. The amplitude of PACAP was calculated as the average of the difference of tension from the bottom to the peak of the trace of SPCs, and the tone was calculated as the average of the tension at the bottom of the trace of SPCs. All experiments were performed under the presence of TTX 1 μ M to eliminate neural effects to muscle contractility.

Ca^{2+} Imaging in Human Tissues

Longitudinal muscle preparations with adherent myenteric layer of human colon (approximately 5-mm square) were prepared by removing the mucosal and circular muscle layers. The preparations were pinned flatly on a Sylgard plate (silicone elastomer, Dow Corning Corporation, Midland, MI) at the bottom of the recording chamber (volume, approximately 1 mL), and superfused with warmed (36°C) physiological salt solution (PSS) at a constant flow rate (2 mL/min) and equilibrated for 60 minutes.

To visualize intracellular Ca^{2+} dynamics in PICs, preparations were incubated in low Ca^{2+} PSS ($[Ca^{2+}]_o = 0.1$ mM) containing 1 to 3 μ M Cal-520 AM (AAT Bioquest Inc) and cremphor EL (0.01 %, Sigma) for 20 to 30 minutes at 35°C, then 10 to 15 minutes at room temperature.¹²

Following incubation, the recording chamber was mounted on the stage of an upright epifluorescence microscope (BX51WI, Olympus, Tokyo, Japan) equipped with a

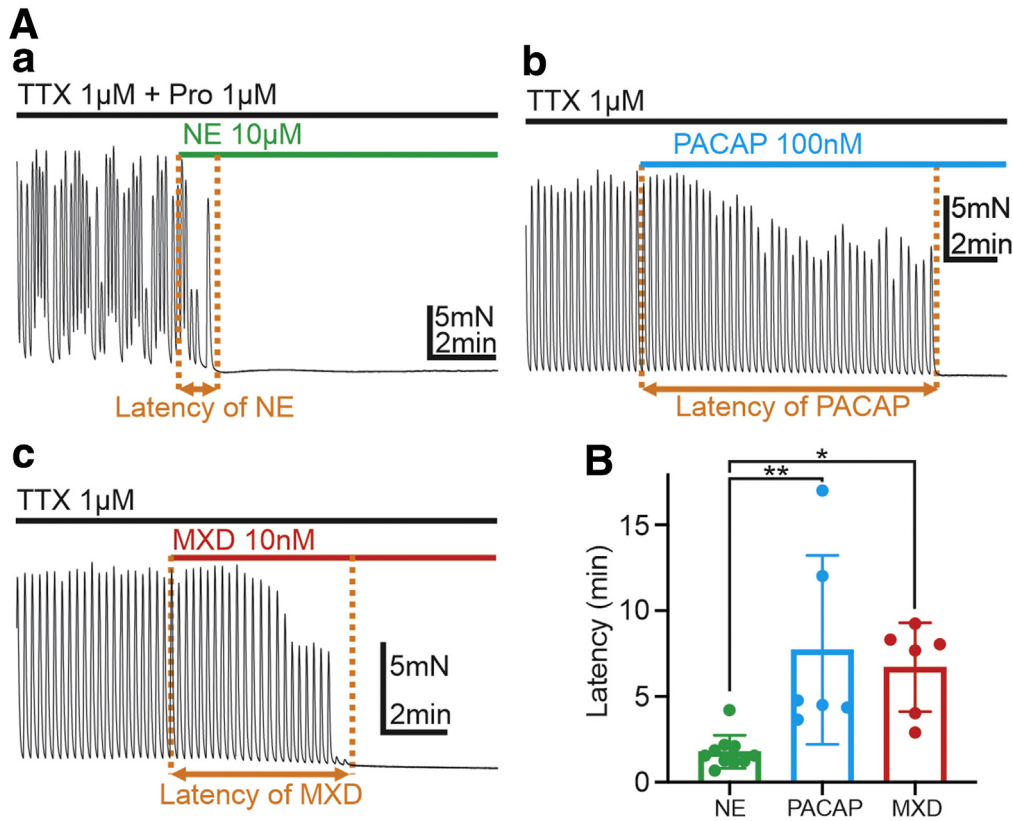


Figure 9. The latency of the response to PAC₁R agonists. *A*, The latency of the response to PAC₁R agonists (PACAP: *Ab*; *n* = 6 and MXD: *Ac*; *n* = 6) was longer than the one to NE (*Aa*; *n* = 10). *B*, Summarized graphs showing the latency of the response to NE, PACAP, and MXD. The responses to PAC₁R agonists were significantly longer than the one to NE. *.05 > *P* ≥ .01; **.01 > *P*. In the graph, boxes, dots, and vertical lines represent means, individual values and standard deviation, respectively.

back-thinned electron multiplying CCD camera (C9100-13, Hamamatsu Photonics, Hamamatsu, Japan). Preparations were superfused with dye-free PSS containing 2.5 mM Ca²⁺, viewed with a water immersion objective

(LUMPlanFL ×40, ×60, Olympus) and illuminated at 495 nm. Fluorescence was captured through a barrier filter above 515 nm, and images were obtained every 100 to 137 ms (frame interval) with an exposure time of 70 to 100 ms using a micro-photoluminescence measurement system (AQUACOSMOS, Hamamatsu Photonics). Relative amplitudes of Ca²⁺ transients were expressed as $\Delta F_t/F_0 = (F_t - F_0)/F_0$, where F_t is the fluorescence generated by an event, and baseline F_0 is the basal fluorescence.

EFS was applied by passing brief currents (50 μ s duration, 10 Hz or 20 Hz, 1 s, supramaximal voltage [approximately 100 V]) between a pair of platinum plate electrodes in the recording chamber using an electronic stimulator (SEN-3301; Nihon Kohden, Tokyo, Japan) and isolators (SS-104; Nihon Kohden, Tokyo, Japan). Neural selectivity of EFS was confirmed by the sensitivity of EFS-induced responses to 1 μ M TTX.

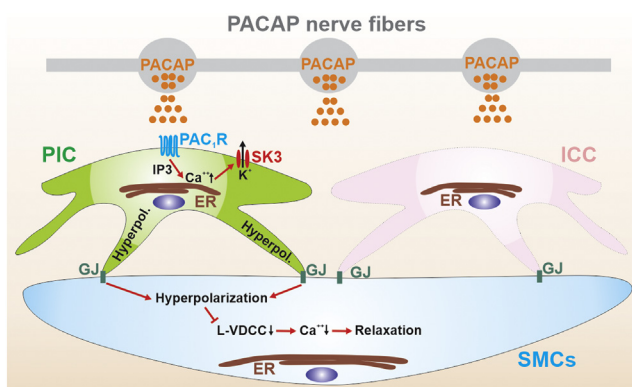


Figure 10. Schematic diagram of PACAP signaling based on this study. PAC₁R is expressed predominantly and plentifully in PIC. PACAP from enteric nerve fibers bind to PAC₁R in PICs, opens SK3 through increasing intracellular [Ca²⁺] by IP3 in PIC and hyperpolarize (Hyperpol.) them. Hyperpolarization of PIC is propagated to SMCs (pale blue cell) via gap junctions (GJ). Hyperpolarization of SMCs reduces the open probability of L-type Ca²⁺ channels (L-VDCC) and decreases intracellular [Ca²⁺], leading to relaxation of SMCs. ICC (pale pink cell) do not seem to be involved in this pathway.

Intracellular Electrical Recordings

A tissue segment of human S colon circular muscles (1 × 3 mm) was pinned to the floor of a recording chamber. The tissue was superfused with warmed (35 °C) and oxygenated Krebs solution, at a constant flow rate of approximately 2 mL/min. Experiments were carried out in the presence of 3 μ M nifedipine to minimize muscle movements. Conventional microelectrode techniques were used to record transmembrane potentials from human colonic muscle strips. Glass capillary microelectrodes (outer diameter, 1.5 mm;

Table 4. Primers for qPCR

Gene name	Primer sequence	Product length, bp	Accession number
<i>Gapdh</i>	F- GCCGATGCCCCCATGTTTGTGA R-GGGTGGCAGTGATGGCATGGAC	178	NM_008084
<i>Adcyap1r1</i>	F-AACGACCTGATGGGCCTAAA R-TGTCATCCAGACTTGGTCCG	153	NM_007407
<i>Vipr1</i>	F-TCAATGGCGAGGTGCAGGCAG R-TGTGTGCTGCACGAGACGCC	127	NM_011703
<i>Vipr2</i>	F- AGGAAGCTGCACTGCACAAGGAA R- GAGCTTGCAGCCAACCCAGGA	159	NM_009511

inner diameter, 0.86 mm; Hilgenberg, Malsfeld, Germany) were filled with KCl 2 M and had tip resistances ranging between 50 and 80 M Ω . Electrical responses were recorded via a high input impedance amplifier (Axoclamp-2B; Axon Instruments, San Jose, CA) and stored on a computer for subsequent analysis and display.

Mechanical Tension Recordings of CM Strips of Human Sigmoid Colon

Immediately after the colorectal resections, pieces of human colonic specimens were dissected out and kept in Krebs solution containing indomethacin 1 μ M cooled in ice to reduce inflammatory responses. Small muscle strips with 10 mm long and 2 mm width along the direction of circular muscle fibers were prepared. Threads were tied around both ends of the strips; one thread was fixed at the bottom of an organ bath chamber, and the other was connected to an isometric force transducer with a bridge amplifier (ADInstruments Ltd, Hasting, UK). Tension was digitized with Digidata 1200 interface (Axon Instruments, Inc, San Jose, CA) and was analyzed with pCLAMP 10 software (Molecular Devices, LLC, San Jose, CA). The strips were perfused at a constant flow rate of 1 mL/min with oxygenized, warmed (36 $^{\circ}$ C) Krebs solution for 1 hour, and then initial tension of 5 to 10 mN was applied. The experimental protocols were started when SPCs and basal tension became stable 1 hour or longer after applying the initial tension. Each of the experimental protocols was applied to one sample, and any multiple experimental protocols were not applied in one single sample. To analyze the responses of SPCs to PACAP and MXD in the specific conditions, 4 parameters of SPCs (AUC, amplitude, tone, and frequency) were measured for 10 minutes after adding PACAP and MXD at the various concentrations. The amplitude of SPCs was calculated as the average of the difference of tension from the bottom to the peak of the trace of SPCs, and the tone was calculated as the average of the tension at the bottom of the trace of SPCs. All experiments were performed under the presence of TTX 1 μ M to eliminate neural effects to muscle contractility.

Solutions and Drugs

Composition of Krebs solution was (mM): Na⁺ 137.5; K⁺ 5.9; Ca²⁺ 2.5; Mg²⁺ 1.2; HCO³⁻ 15.5; H₂PO₄⁻ 1.2; Cl⁻ 134;

glucose 11.5. The solution was bubbled with 95% O₂ and 5% CO₂ and the pH of solution was maintained at 7.3 to 7.5. Reagents used in this study were: PACAP-38 (PACAP in this study), PACAP 6-38 (selective PAC₁R antagonist), Maxadilan (selective PAC₁R agonist), and VIP from BACHEM (Torrance, CA); MRS2500 (selective P2Y₁ purinoceptor antagonist) and MRS2365 (selective P2Y₁ purinoceptor agonist) from Tocris Bioscience (Ellisville, MO, USA); TTX from Wako (Osaka, Japan) or Abcam (Cambridge, UK); Apamin from Peptide Institute (Osaka, Japan) or Santa Cruz Biotechnology (Santa Cruz, CA); Atropine and L-NNA from MilliporeSigma (Burlington, MA).

Statistical Analysis

Experimental values were represented with means \pm standard deviation. All statistical analysis were performed with GraphPad Prism. Statistical significance was tested with 1-way analysis of variance or paired *t* test, and probabilities of less than 5% (*P* < .05) were considered significant.

References

1. Iino S, Horiguchi K, Horiguchi S, Nojyo Yoshiaki. c-Kit-negative fibroblast-like cells express platelet-derived growth factor receptor alpha in the murine gastrointestinal musculature. *Histochem Cell Biol* 2009; 131:691–702.
2. Kurahashi M, Nakano Y, Henning GW, Ward SM, Sanders KM. Platelet-derived growth factor receptor α -positive cells in the tunica muscularis of human colon. *J Cell Mol Med* 2012;16:1397–1404.
3. Komuro T, Seki K, Horiguchi K. Ultrastructural characterization of the interstitial cells of Cajal. *Arch Histol Cytol* 1999;62:295–316.
4. Sanders KM, Koh SD, Ro S, Ward SM. Regulation of gastrointestinal motility—insights from smooth muscle biology. *Nat Rev Gastroenterol Hepatol* 2012;9:633–645.
5. Sanders KM, Kito Y, Hwang SJ, Ward SM. Regulation of gastrointestinal smooth muscle function by interstitial cells. *Physiology* 2016;31:316–326.
6. Kurahashi M, Zheng H, Dwyer L, Ward SM, Koh SD, Sanders KM. A functional role for the ‘fibroblast-like cells’ in gastrointestinal smooth muscle. *J Physiol* 2011; 589:697–710.

7. Kurahashi M, Mutafova-Yambolieva V, Koh SD, Sanders KM. Platelet-derived growth factor receptor- α -positive cells and not smooth muscle cells mediate purinergic hyperpolarization in murine colonic muscles. *Am J Physiol Cell Physiol* 2014;307:C561–C570.
8. Baker SA, Hennig GW, Ward SM, Sanders KM. Temporal sequence of activation of cells involved in purinergic neurotransmission in the colon. *J Physiol* 2015;593:1945–1963.
9. Kurahashi M, Kito Y, Baker SA, Jennings LK, Dowers JGR, Koh SD, Sanders KM. A novel post-synaptic signal pathway of sympathetic neural regulation of murine colonic motility. *FASEB J* 2020;34:5563–5577.
10. Gallego D, Hernández P, Clavé P, Jiménez M. P2Y1 receptors mediate inhibitory purinergic neuromuscular transmission in the human colon. *Am J Physiol Gastrointest Liver Physiol* 2006;291:G584–G594.
11. Hwang SJ, Blair PJ, Durnin L, Mutafova-Yambolieva V, Sanders KM, Ward SM. P2Y1 purinoreceptors are fundamental to inhibitory motor control of murine colonic excitability and transit. *J Physiol* 2012;590:1957–1972.
12. Kurahashi M, Kito Y, Hara M, Takeyama H, Sanders KM, Hashitani H. Norepinephrine has dual effects on human colonic contractions through distinct subtypes of alpha 1 adrenoceptors. *Cell Mol Gastroenterol Hepatol* 2020;10:658–671.e1.
13. Ha SE, Lee MY, Kurahashi M, Wei L, Jorgensen BG, Park C, Park PJ, Redelman D, Sasse KC, Becker LS, Sanders KM, Ro S. Transcriptome analysis of PDGFR α + cell hyperplasia. *PLoS One* 2017;12:e0182265.
14. Miyata A, Arimura A, Dahl RR, Minamino N, Uehara A, Jiang L, Culler MD, Coy DH. Isolation of a novel 38 residue-hypothalamic polypeptide which stimulates adenylate cyclase in pituitary cells. *Biochem Biophys Res Commun* 1989;164:567–574.
15. Arimura A. Pituitary adenylate cyclase activating polypeptide (PACAP): discovery and current status of research. *Regul Pept* 1992;37:287–303.
16. Ishihara T, Shigemoto R, Mori K, Takahashi K, Nagata S. Functional expression and tissue distribution of a novel receptor for vasoactive intestinal polypeptide. *Neuron* 1992;8:811–819.
17. Pisegna JR, Wank SA. Molecular cloning and functional expression of the pituitary adenylate cyclase-activating polypeptide type I receptor. *Proc Natl Acad Sci U S A* 1993;90:6345–6349.
18. Vaudry D, Falluel-Mrel A, Bourgault S, Basille M, Burel D, Wurtz O, Fournier A, Chow BKC, Hashimoto H, Galas L, Vaudry H. Pituitary adenylate cyclase-activating polypeptide and its receptors: 20 years after the discovery. *Pharmacol Rev* 2009;61:283–357.
19. Schworer H, Clemens A, Katsoulis S, Kohler H, Creutzfeldt W, Schmidt WE. Pituitary adenylate cyclase-activating peptide is a potent modulator of human colonic motility. *Scand J Gastroenterol* 1993;28:625–632.
20. Serio R, Alessandro M, Zizzo MG, Tamburello MP, Mulè F. Neurotransmitters involved in the fast inhibitory junction potentials in mouse distal colon. *Eur J Pharmacol* 2003;460:183–190.
21. Zizzo MG, Mulè F, Serio R. Mechanisms underlying the inhibitory effects induced by pituitary adenylate cyclase-activating peptide in mouse ileum. *Eur J Pharmacol* 2005;521:133–138.
22. Lee MY, Park C, Berent RM, Park PJ, Fuchs R, Syn H, Chin A, Townsend J, Benson CC, Redelman D, Shen T-W, Park JK, Miano JM, Sanders KM, Ro S. Smooth muscle cell genome browser: enabling the identification of novel serum response factor target genes. *PLoS One* 2015;10:e0133751.
23. Lee MY, Ha SE, Park C, Park PJ, Fuchs R, Wei L, Jorgensen BG, Redelman D, Ward SM, Sanders KM, Ro S. Transcriptome of interstitial cells of Cajal reveals unique and selective gene signature. *PLoS One* 2017;12:e0176031.
24. Blechman J, Levkowitz G. Alternative splicing of the pituitary adenylate cyclase-activating polypeptide receptor PAC1: mechanisms of fine tuning of brain activity. *Front Endocrinol (Lausanne)* 2013;4:55.
25. Rumessen JJ, Thuneberg L, Mikkelsen HB. Plexus muscularis profundus and associated interstitial cells. II. Ultrastructural studies of mouse small intestine. *Anat Rec* 1982;203:129–146.
26. Horiguchi K, Komuro T. Ultrastructural observations of fibroblast-like cells forming gap junctions in the W/W(nu) mouse small intestine. *J Auton Nerv Syst* 2000;80:142–147.
27. Kurahashi M, Nakano Y, Peri LE, Townsend JB, Ward SM, Sanders KM. A novel population of sub-epithelial platelet-derived growth factor receptor α -positive cells in the mouse and human colon. *Am J Physiol Gastrointest Liver Physiol* 2013;304:G823–G834.
28. Portbury AL, McConalogue K, Furness JB, Young HM. Distribution of pituitary adenylate cyclase activating peptide (PACAP) immunoreactivity in neurons of the guinea-pig digestive tract and their projections in the ileum and colon. *Cell Tissue Res* 1995;279:385–392.
29. Rettenbacher M, Reubi JC. Localization and characterization of neuropeptide receptors in human colon. *Naunyn-Schmiedeberg Arch Pharmacol* 2001;364:291–304.
30. Miampamba M, Germano PM, Arli S, Wong HH, Scott D, Tache Y, Pisegna JR. Expression of pituitary adenylate cyclase-activating polypeptide and PACAP type 1 receptor in the rat gastric and colonic myenteric neurons. *Regul Pept* 2002;105:145–154.
31. Peri LE, Sanders KM, Mutafova-Yambolieva VN. Differential expression of genes related to purinergic signaling in smooth muscle cells, PDGFR α -positive cells, and interstitial cells of Cajal in the murine colon. *Neurogastroenterol Motil* 2013;25:e609–e620.
32. Uhlen M, Fagerberg L, Hallstrom BM, Lindskog C, Oksvold P, Mardinoglu A, Sivertsson A, Kampf C, Sjostedt E, Asplund A, Olsson I, Edlund K, Lundberg E, Navani S, Sztybel CA, Odeberg J, Djureinovic D, Takanen JO, Hober S, Alm T, Edqvist PH, Berling H, Tegel H, Mulder J, Rockberg J, Nilsson P, Schwenk JM, Hamsten M, Feltzen K, Forsberg M, Persson L, Johansson F, Zwahlen M, von Hije G, Nielsen J,

- Ponten F. Proteomics. Tissue-based map of the human proteome. *Science* 2015;347:1260419.
33. Piascik MT, Perez DM. Alpha1-adrenergic receptors: new insights and directions. *J Pharmacol Exp Ther* 2001; 298:403–410.
 34. Wood JD. The enteric purinergic P2Y1 receptor. *Curr Opin Pharmacol* 2006;6:564–570.
 35. Parker I, Ito Y, Kuriyama H, Miledi R. Beta-adrenergic agonists and cyclic AMP decrease intracellular resting free-calcium concentration in ileum smooth muscle. *Proc R Soc Lond B Biol Sci* 1987;230:207–214.
 36. Bai Y, Sanderson MJ. Airway smooth muscle relaxation results from a reduction in the frequency of Ca²⁺ oscillations induced by a cAMP-mediated inhibition of the IP₃ receptor. *Respir Res* 2006;7:34.
 37. Kishi M, Takeuchi T, Suthamnatpong N, Ishii T, Nishio H, Hata F, Takewaki T. VIP- and PACAP-mediated non-adrenergic, noncholinergic inhibition in longitudinal muscle of rat distal colon: involvement of activation of charybdotoxin- and apamin-sensitive K⁺ channels. *Br J Pharmacol* 1996;119:623–630.
 38. Matsuda NM, Miller SM. Non-adrenergic non-cholinergic inhibition of gastrointestinal smooth muscle and its intracellular mechanism(s). *Fundam Clin Pharmacol* 2010;24:261–268.
 39. Laburthe M, Couvineau A. Molecular pharmacology and structure of VPAC receptors for VIP and PACAP. *Regul Pept* 2002;108:165–173.
 40. Eiden LE, Emery AC, Zhang L, Smith CB. PACAP signaling in stress: insights from the chromaffin cell. *Pflugers Arch* 2018;470:79–88.
 41. Hamilton TG, Klinghoffer RA, Corrin PD, et al. Evolutionary divergence of platelet-derived growth factor alpha receptor signaling mechanisms. *Mol Cell Biol* 2003;23:4013–4025.
 42. Zhu MH, Kim TW, Ro S, et al. A Ca²⁺-activated Cl⁻ conductance in interstitial cells of Cajal linked to slow wave currents and pacemaker activity. *J Physiol* 2009; 587:4905–4918.
 43. Koh SD, Dick GM, Sanders KM. Small-conductance Ca²⁺-dependent K⁺ channels activated by ATP in murine colonic smooth muscle. *Am J Physiol* 1997; 273:C2010–C2021.
 44. Baker SA, Leigh WA, Valle GD, De Yturriaga IF, Ward SM, Cobine CA, Drumm BT, Sanders KM. Ca²⁺ signaling driving pacemaker activity in submucosal interstitial cells of Cajal in the murine colon. *Elife* 2021; 10:e64099.
 45. Leigh WA, Valle GD, Kamran SA, Drumm BT, Tavakkoli A, Sanders KM, Baker SA. A high throughput machine-learning driven analysis of Ca²⁺ spatio-temporal maps. *Cell Calcium* 2020;91:102260.

Received February 6, 2022. Accepted May 5, 2022.

Correspondence

Address correspondence to: Masaaki Kurahashi, MD, PhD, 200 Hawkins Dr, University of Iowa, Department of Internal Medicine, Division of Gastroenterology and Hepatology, Iowa City, IA 52242. e-mail: masaaki-kurahashi@uiowa.edu; tel: (319) 467-8963.

CRedit Authorship Contributions

Masaaki Kurahashi, MD, PhD (Conceptualization: Lead; Data curation: Lead; Formal analysis: Lead; Funding acquisition: Lead; Investigation: Lead; Methodology: Lead; Project administration: Lead; Resources: Lead; Software: Lead; Supervision: Lead; Validation: Lead; Visualization: Lead; Writing – original draft: Lead; Writing – review & editing: Lead)

Salah A. Baker, PhD (Data curation: Supporting; Formal analysis: Supporting; Investigation: Supporting; Methodology: Supporting; Software: Supporting; Writing – review & editing: Supporting)

Yoshihiko Kito, PhD (Data curation: Supporting; Formal analysis: Supporting; Investigation: Supporting; Methodology: Supporting; Software: Supporting; Writing – review & editing: Supporting)

Allison Bartlett (Data curation: Supporting; Investigation: Supporting; Writing – review & editing: Supporting)

Masayasu Hara, MD & PhD (Data curation: Supporting; Investigation: Supporting; Writing – review & editing: Supporting)

Hiromitsu Takeyama, MD & PhD (Data curation: Supporting; Investigation: Supporting; Writing – review & editing: Supporting)

Hikaru Hashitani, MD & PhD (Data curation: Supporting; Formal analysis: Supporting; Methodology: Supporting; Resources: Supporting; Software: Supporting; Supervision: Supporting; Validation: Supporting; Visualization: Supporting; Writing – review & editing: Supporting)

Kenton M. Sanders, PhD (Funding acquisition: Equal; Project administration: Supporting; Writing – original draft: Equal; Writing – review & editing: Equal)

Conflicts of interest

The authors disclose no conflicts.

Funding

This study was funded by the National Institute of Diabetes and Digestive and Kidney Diseases (NIDDK) Grant R01-DK-091336